DOI: 10.1111/cgf.13275

Pacific Graphics 2017
J. Barbic, W.-C. Lin, and O. Sorkine-Hornung
(Guest Editors)

Volume 36 (2017), Number 7

$\mathscr{L}0$ Gradient-Preserving Color Transfer

Dong Wang [1] and Changqing Zou † [2,3] and Guiqing Li [4] and Chengying Gao [5] and Zhuo Su [5] and Ping Tan [3]

[1] College of Mathematics and Informatics, South China Agricultural University, China
[2] College of Computer Science and Technology, Hengyang Normal Univerisity, China
[3] School of Computing Science, Simon Fraser University, Canada
[4] School of Computer Science & Engineering, South China University of Technology, China
[5] School of Data and Computer Science, National Engineering Research Center of Digital Life, Sun Yat-Sen University, China

(a) (b) (c) (d) (e)

Figure 1: *Color transfer comparisons. (a) Source image; (b) target color palette; (c) Chang et al.'s method [CFL*15]; (d) gradient-preserving method [XM09]; and (e) $\mathscr{L}0$ gradient-preserving method.*

Abstract

This paper presents a new two-step color transfer method which includes color mapping and detail preservation. To map source colors to target colors, which are from an image or palette, the proposed similarity-preserving color mapping algorithm uses the similarities between pixel color and dominant colors as existing algorithms and emphasizes the similarities between source image pixel colors. Detail preservation is performed by an $\mathscr{L}0$ gradient-preserving algorithm. It relaxes the large gradients of the sparse pixels along color region boundaries and preserves the small gradients of pixels within color regions. The proposed method preserves source image color similarity and image details well. Extensive experiments demonstrate that the proposed approach has achieved a state-of-art visual performance.

CCS Concepts

•***Computer Graphics*** → *Image & Video; Image/Video Editing;*

1. Introduction

Color transfer is an image editing technique that produces a new image by combining source image contents with the color style of a target image or color palette. It is present in various applications in image and video processing tasks [TJT05, SPLM15]. For instance, a cloudy day photo may be rendered as a sunny day photo using this color transfer technique. Such an appearance manipulation technique can expedite image and video editing processing.

When applying target colors to a source image, a successful color transfer algorithm must preserve both source image details and color similarity. Previous methods usually employ gradient-preserving constraints [XM09, PKD07] or implicit filtering schemes [YPCL13, SZL*14] to maintain source image details. Gradient-preserving based methods generally try to make resulting image pixels share the same gradient fields as those in the source image. These techniques work well only when all colors follow

† Corresponding author:aaronzou1125@gmail.com

similar transformations. When neighboring pixel transformations are significantly different, a global gradient preservation forced by these algorithms usually results in visual artifacts in the resulting image, such as those seen around the cherry tomato boundaries in Fig. 1(d). Implicit filtering schemes attempt to preserve original color similarities among local pixels and have the same problems as gradient-preserving based methods.

To build the mapping between target and source image colors, global color mapping is usually performed under an assumption that source image and target image have similar global color distributions [RAGS01, PKD05, PKD07, XM09]. A typical limitation of those algorithms is that source image color similarity is not preserved well when source and target color statistics differ greatly. Dominant color based algorithms [TJT05, RDG11, YPCL13, CFL*15] may alleviate this problem using a two-stage color mapping strategy which first obtains the mapping from source image dominant colors to target image dominant colors and then propagates that mapping to all source image pixels. However, pixel color similarity may be destroyed when color consistency of source dominant colors and target dominant colors is large. A typical example is shown in Fig. 1(c) where there are two visually primary colors, red and orange, in the cherry tomatoes. But there is one primary color, yellow, in the source image in Fig. 1(a). Pixel color similarity is not preserved in this case.

This paper proposes a new color transfer method to better preserve image details and color similarity. The improved detail preservation performance is obtained by a new algorithm, which is described as $\mathscr{L}0$ gradient-preserving based model. It differs from present gradient-preserving models which treat all pixel gradients equally during color transfer. The proposed $\mathscr{L}0$ gradient-preserving model forces color region pixel gradients in resulting image to maintain the original values in the source image. It relaxes this constraint for pixels along color region boundaries. The experiments demonstrate that the $\mathscr{L}0$ gradient-preserving model produces visually better results compared to previous gradient-preserving models.

For color mapping, a dominant color based model is proposed which uses similarity-preserving color mapping. It requires that source image pixels with similar colors follow similar transformations, which makes the approach slightly affected by color consistency of dominant colors. Pixel similarity-preserving constraints will result in a large-scale non-sparse optimization solution, and the algorithm uses a hierarchical scheme to simplify computation. This hierarchy is achieved by introducing source image super-pixels as samples. The experiments demonstrate the proposed algorithm is effective to improve the prevailing dominant color based color mapping model.

2. Related Work

This section summarizes research related to color mapping, detail preservation and several $\mathscr{L}0$-norm optimization techniques.

Color mapping. Color mapping establishes color correspondences between source image and target image, and transforms source image colors into target image colors. Algorithms related to color mapping can be roughly divided into two categories: global mapping and local mapping. In global mapping algorithms, color statistics are usually calculated by taking into account all image pixels [PKD05, PKD07, XM09, RAGS01, SZL*14, XLH15]. Reinhard et al. mapped target image color mean and variance to source image color mean and variance in [RAGS01]. Pitie et al. [PKD05,PKD07] proposed an N-dimensional probability density function (PDF) transfer approach. Continuous mapping transforms source image colors into a new color ensemble exhibiting a similar PDF as the target image colors. Xiao and Ma [XM09] used a global histogram matching algorithm forcing the color histograms of the resulting image and the target image to be the same. A similar color histogram matching based color mapping scheme was also used in [SZL*14]. In addition, Nguyen et al. [NRS15] projected a high-dimensional color space of an object to a lower-dimensional manifold with varying density from labeled Internet examples. Luan et al. [LPSB17] introduced a deep-learning approach to map target image colors to source image.

In general, the performance of the global algorithms depends on the similarities between target image color distribution and source image color distribution. Visually ideal results can be achieved when the color statistics of source image and target image are similar. They are likely to produce unnatural and saturated results when the two color statistics differ significantly. For example, the algorithm in [PKD05] might stretch pixel color values in the source image and result in content distortions when the PDFs from the source image and target image are not similar; The algorithm in [RAGS01] is also likely to produce slight grain effects and serious color distortions when source image color variances differ greatly from target image color variances [SZL*14].

Several local mapping algorithms were proposed to alleviate the limitations of global algorithms. In these algorithms, color transfer occurs in the presence of color correspondences and spatial relations [TJT05]. The strategy was to first obtain the correspondences of representative colors (dominant colors in [TJT05, TJT07, YPCL13, CFL*15], feature point colors in [HLKK14], and image patch colors in [HSGL11]) from source image to target image, then propagate the correspondences to all the pixel colors of source image by using techniques such as GMM and radial basis function interpolation.

This technique also uses dominant color based color mapping scheme to perform a local color transfer. Different from present algorithms which only maintain the similarities between pixel colors and dominant colors, our color mapping strategy additionally requires that source image pixels with similar colors follow similar transformations, which makes the approach slightly affected by color consistency of dominant colors.

Detail preservation. After color mapping, some image details may be lost or changed. It often happens where neighboring pixels with similar colors are mapped in a different way. Additional constraints are usually used to preserve the image details in previous methods.

The methods in [PKD05, PKD07, XM09, WDK*13] introduced gradient-preserving constraints into color transfer. Other works in [WYW*10, WYX11, NKB14] also employed schemes similar to gradient-preserving. Pouli et al. [PR11] applied bilateral

filters [TM98] onto color mapping results to produce smooth-looking image results. Bonneel et al. [BSPP13] added a spatial filtering step onto color mapping results to preserve video details. Rabin et al. proposed a nonlocal Yaroslavsky spatial filter in [RDG11] to suppress artifacts, while preserving image details. Su et al. [SZL*14] exploited an iterative probabilistic color mapping approach, equipped with a self-learning filtering scheme and a multi-scale detail manipulation procedure minimizing the normalized Kullback-Leibler distance. Our method differs from these detail preservation schemes mentioned above. It employs an $\mathscr{L}0$ gradient-preserving model which confines the gradient change count to achieve detail preservation.

$\mathscr{L}0$-norm optimization. Although $\mathscr{L}0$ gradient-preserving has not been used in color transfer scenario, there are some instances which leverage $\mathscr{L}0$-norm optimization in visual computing applications. For instance, He et al. [HS13] proposed a solution for mesh denoising via $\mathscr{L}0$ gradient minimization. Zhang et al. [ZDL13, DZ13] introduced a wavelet-based $\mathscr{L}0$ minimization method for image restoration. Zhang et al. [ZZZG14] proposed to use $\mathscr{L}0$ minimization to provide a sparse basis for image recovery. Cheng et al. [CZL14] solved a fused coordinate descent problem for feature preserving surface smoothing through $\mathscr{L}0$ gradient minimization. Shen et al. decomposed an image into a base layer and a detail layer by combining L_1 fidelity and $\mathscr{L}0$ gradient minimization in [SCHP12].

Our $\mathscr{L}0$-norm optimization scheme is related to the work in [XLXJ11, QL15]. They proposed an $\mathscr{L}0$ gradient minimization based optimization framework to obtain an edge-preserving image smoothing task. Their algorithm enforced pixel gradients within color regions as zeros and preserved the large gradients for the pixels along region boundaries. The $\mathscr{L}0$ gradient-preserving optimization scheme differs from this in that it requires the pixels maintaining original gradients to be as numerous as possible. The algorithm results in pixel gradients within color regions often preserving the original value (i.e., the gradient value of the corresponding source image pixel), and pixel gradients located at color region boundaries probably having a great difference from their original values.

3. Definition of Terms

Color similarity. Color similarity of two colors is inversely proportional to their distance. Specifically, given RGB colors $\mathbf{c}_i$ and $\mathbf{c}_j$, their similarity is defined by $s(\mathbf{c}_i,\mathbf{c}_j) = exp(-d_{ij}^2/\sigma)$, where $d_{ij} = \| \mathbf{c}_i - \mathbf{c}_j \|$ is the Euclidean distance of the two colors and σ is the covariance parameter which is usually set to 0.005. A large $s(\mathbf{c}_i,\mathbf{c}_j)$ indicates high similarity.

Set-wise color similarity. We introduce this notion to measure the similarity between two sets of colors. Concretely, let $\mathbf{A} = \{\mathbf{c}_a(1),...,\mathbf{c}_a(M)\}$ and $\mathbf{B} = \{\mathbf{c}_b(1),...,\mathbf{c}_b(N)\}$, where M and N respectively denote the element number of the two color sets. Their set-wise color similarity $S_{\mathbf{A},\mathbf{B}}$, which is a $M \times N$ matrix, records all the color similarity between all color pairs $\mathbf{c}_a(i) \in \mathbf{A}$ and $\mathbf{c}_b(j) \in \mathbf{B}$. Specifically, entry $S_{(\mathbf{A},\mathbf{B})}(i,j) = s(\mathbf{c}_a(i),\mathbf{c}_b(j))$. Set-wise color similarity between $\mathbf{A}$ and itself is denoted by $S_{\mathbf{A}}$.

Color consistency. Color consistency is used to measure the matching degree between source image dominant colors and target image dominant colors under the given mapping. Set source dominant colors $\mathbf{A} = \{\mathbf{c}_a(1),...,\mathbf{c}_a(N_S)\}$ and target dominant colors $\mathbf{B} = \{\mathbf{c}_b(1),...,\mathbf{c}_b(N_T)\}$. $\pi : \{1,...,N_S\} \to \{1,...,N_T\}$ is the mapping from A to B, namely, $\mathbf{c}_a(i)$ is mapped to $\mathbf{c}_b(\pi(i))$. Color consistency of π is then defined as

$$CC(\pi,\ \mathbf{A},\mathbf{B}) = \sum_{i=1}^{N_S} \sum_{j=i+1}^{N_S} (|S_{\mathbf{A}}(i,j) - S_{\mathbf{B}}(\pi(i),\pi(j))|). \quad (1)$$

Small $CC(\pi,A,B)$ indicates a strong matching, and vice versa.

Similarity-preserving color mapping. Let a color mapping procedure recolor I_S to I_M, namely, color $I_S(i)$ of pixel i is changed to $I_M(i)$. If always having $|I_M(i) - I_M(j)| \approx 0$ for all pixel pairs i, j in I_S satisfying $s(I_S(i),I_S(j)) \approx 1$, we then say the color mapping procedure is similarity-preserving.

Color region. A connected pixel region where pixels have similar colors (i.e., in this region, color similarity between pixels is large) is called a color region. The boundary of this region is called region boundary. The pixel gradients within a color region are small and those along region boundaries are large. The regions depicting cherry tomatoes in Fig. 1 are typical color regions.

4. Overview

Given an input pair: source image $\mathbf{I}_S$ and target image/palette $\mathbf{I}_T$, the framework contains two sequential procedures: a similarity-preserving color mapping procedure followed by an $\mathscr{L}0$ gradient-preserving based detail restoration procedure. The color mapping procedure generates an intermediate image $\mathbf{I}_M$ with $\mathbf{I}_S$ content and $\mathbf{I}_T$ tone. The detail restoration procedure produces a detail-preserving resulting image $\mathbf{I}_R$ with $\mathbf{I}_M$ and gradients $\nabla\mathbf{I}_S$ as the input.

The color mapping procedure extracts two sets of dominant colors D_S and D_T from $\mathbf{I}_S$ and $\mathbf{I}_T$ by clustering pixel colors in the respective image. A color mapping π is then established from D_S to D_T. $\mathbf{I}_S$ is segmented into superpixels U to obtain effective samples. According to the mapping π and clusters, the initial color mapping (offset color vector) is obtained for those superpixels. It is further optimized by color similarity-preserving constraint. Using this optimal color mapping of those superpixels, the color mapping for all pixels is computed to generate image $\mathbf{I}_M$.

Color mapping procedure output $\mathbf{I}_M$ usually does not preserve $\mathbf{I}_S$ details well. This is due to the optimal color mapping scheme not always accurately preserving the color similarity between two superpixels. When each superpixel transformation propagates to its pixels, the boundary pixels of neighbor superpixels may have different color offset vectors, which may lead to different gradient values between $\mathbf{I}_M$ and $\mathbf{I}_S$. If the colors of two neighboring superpixels are very different, this effect is unnoticeable because the boundary is also image edge and does not represent image details. Otherwise gradient values rectification is required. The detail restoration procedure takes $\mathbf{I}_M$ and $\mathbf{I}_S$ gradients as the input and uses a $\mathscr{L}0$-norm gradient preserving model to iteratively optimize $\mathbf{I}_M$ pixel colors to strengthen the consistence of pixel gradients in $\mathbf{I}_M$ and $\mathbf{I}_S$. The scheme results in most pixels in $\mathbf{I}_R$

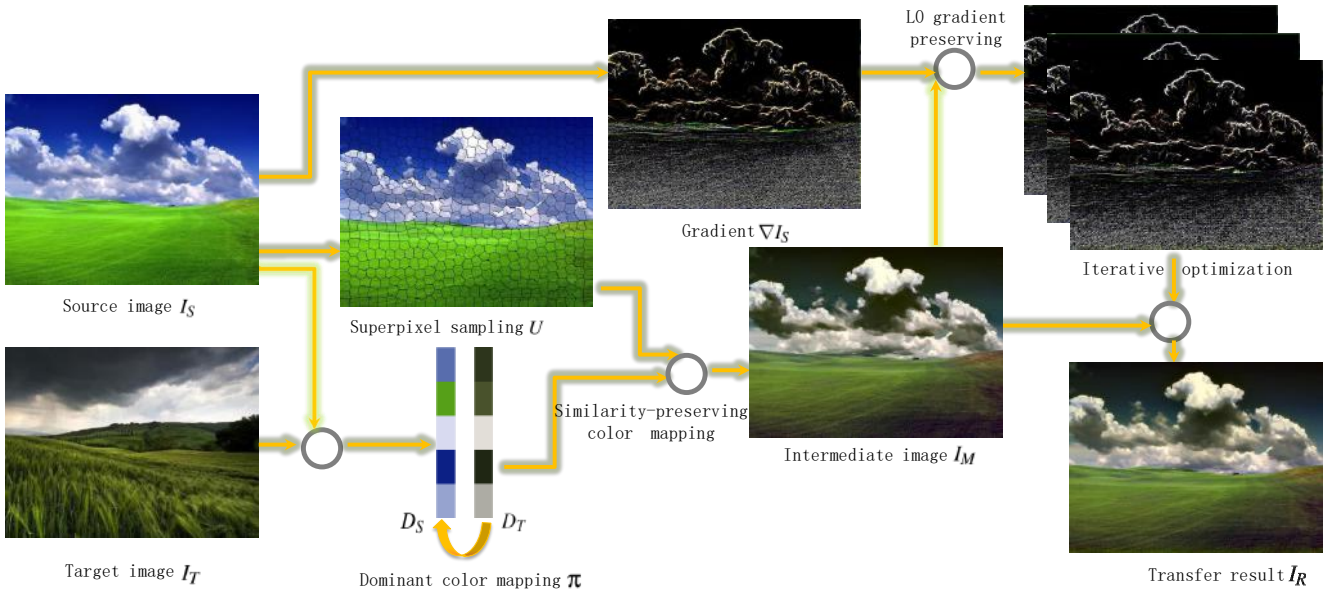

Figure 2: *The flowchart of our approach. Given a source image $\mathbf{I}_S$ and a target image $\mathbf{I}_T$, our approach first generates an intermediate image $\mathbf{I}_M$ through a similarity-preserving color mapping model, and then produces the resulting image $\mathbf{I}_R$ by an $\mathscr{L}0$ gradient-preserving algorithm.*

having the same gradients as the corresponding pixels in $\mathbf{I}_S$. This is accomplished by loosening the gradients of these pixels along the region boundaries. $\mathscr{L}0$ gradient-preserving based detail restoration procedure is described in Section 5. The entire procedure is illustrated in Fig. 2.

5. Similarity-preserving Color Mapping Model

D_S in $\mathbf{I}_S$ and D_T in $\mathbf{I}_T$ are obtained by K-means clustering [Mac67] in RGB color space for $\mathbf{I}_S$ and $\mathbf{I}_T$ separately. Each cluster center $\mathbf{x}$ is selected as a dominant color entity. The dominant colors of $\mathbf{I}_S$ and $\mathbf{I}_T$ are represented respectively as $D_S = \{\mathbf{d}_S(1),\cdots,\mathbf{d}_S(i),\cdots,\mathbf{d}_S(n_S)\}$ and $D_T = \{\mathbf{d}_T(1),\cdots,\mathbf{d}_T(i),\cdots,\mathbf{d}_T(n_T)\}$, where n_S and n_T are the total number of DCs in $\mathbf{I}_S$ and $\mathbf{I}_T$ respectively. With an even probability distribution of all the colors in D_s or D_t as weights, Earth Moving Distance (EMD) algorithm [RG00] is adopted to compute the optimal flow from D_s to D_t, which builds a mapping π from D_S to D_T. The mapping can also be built interactively especially when target image is a palette. For example, given a dominant color, $\mathbf{d}_S(i)$, its corresponding target dominant color can be represented by $\mathbf{d}_T(\pi(i))$.

To transfer each pixel's color in $\mathbf{I}_S$, an initiative solution is a *hard* mapping strategy that makes pixel colors within the common color cluster follow a mapping consistent with the corresponding dominant color. Each pixel would have the same offset color vector as the corresponding dominant color. This hard strategy will probably fail to preserve pixel color similarity in $\mathbf{I}_M$. For example, two close colors in $\mathbf{I}_S$, $\mathbf{c}_i$ and $\mathbf{c}_j$, in RGB space probably correspond to two different dominant colors. It usually results in different color mapping modes and detroys color similarity between $\mathbf{c}_i$ and $\mathbf{c}_j$. Fig. 3(c) is an example of a resulting intermediate image $\mathbf{I}_M$ obtained via this hard mapping strategy. Color similarity changed significantly compared to the source image in Fig. 3(b).

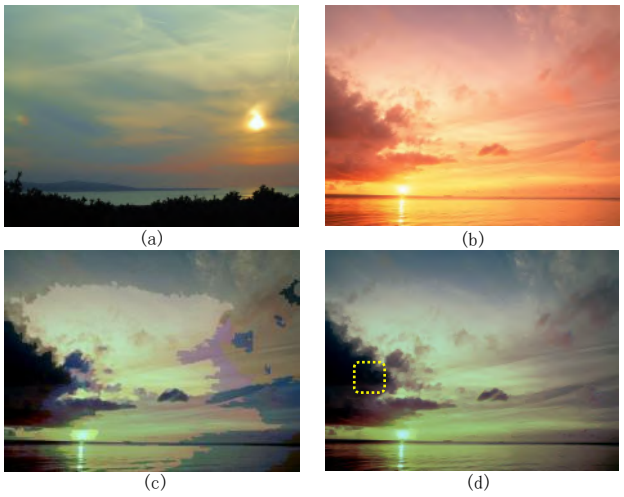

Figure 3: *Color mapping. (a) Target image; (b) source image; (c) hard color mapping result; and (d) soft color mapping result. The intermediate image $\mathbf{I}_M$ from the soft color mapping strategy has fewer color blocks than that from the hard color mapping strategy.*

A *soft* mapping strategy based on similarity-preserving constraint is proposed to address the problems generated by hard mapping. It computes an optimal offset color vector for each pixel in $\mathbf{I}_S$ to preserve the color similarity of any two pixels in $\mathbf{I}_S$, especially for those pixels with high similarity. The soft mapping strategy takes two factors into account: (1) the difference between the expected offset color vector of a pixel in $\mathbf{I}_S$ and the hard mapping one should be related to the similarity between that pixel

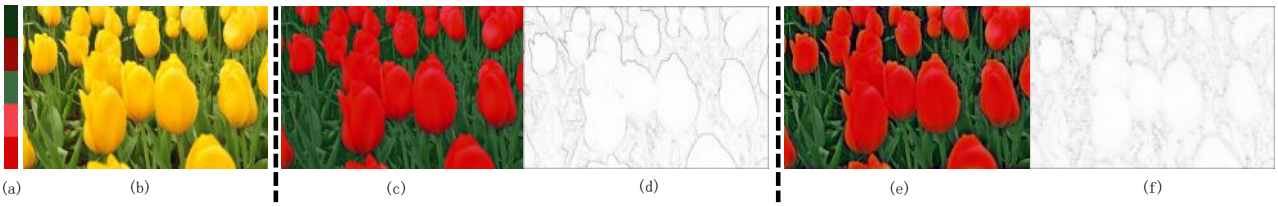

Figure 4: *Detail preservation. The proposed $\mathscr{L}0$ gradient-preserving model and gradient-preserving model were applied to the same input data. (a) Target color palette; (b) source image; (c) $\mathscr{L}0$ gradient-preserving result; (d) gradient difference between (a) and (c); (e) gradient-preserving result; (f) gradient difference between (a) and (e). Large gray value indicates large gradient difference.*

color and its corresponding dominant color; and (2) two color similar pixels should have an analogous offset color vector to preserve their similarity. An optimization algorithm is employed to implement the soft mapping strategy. To achieve efficient color mapping, superpixel level optimization rather than pixel level optimization is performed by determining an optimal offset color vector for all the pixels within a superpixel.

Source image $\mathbf{I}_S$, which contains M pixels, is segmented into N superpixels U by the algorithm in [LTRC11]. Given a superpixel $U(k)$, suppose the majority of its pixel colors belong to the cluster $\tilde{y}$ with dominant color $\mathbf{d}_S(i_k)$, the offset color vector $\hat{\mathbf{g}}_{\tilde{y}}$ of the dominant color $\mathbf{d}_S(i_k)$ can be computed by $\mathbf{d}_T(\pi(i_k)) - \mathbf{d}_S(i_k)$. The objective function computing the optimal offset color vectors of the N superpixels $\{\mathbf{g}'_1, \mathbf{g}'_2, ..., \mathbf{g}'_N\}$ can then be defined as

$$\underset{\{\mathbf{g}'_1,\mathbf{g}'_2,...,\mathbf{g}'_N\}}{\operatorname{argmin}} \sum_{k=1}^{N} [s(\mathbf{u}_k, \mathbf{d}_S(\tilde{y}))(\mathbf{g}'_k - \hat{\mathbf{g}}_{\tilde{y}})^2 + \lambda \sum_{l=1}^{N} (s(\mathbf{u}_k, \mathbf{u}_l)(\mathbf{g}'_k - \mathbf{g}'_l)^2)], \tag{2}$$

where N is the superpiexl number in U, $\mathbf{u}_k$ ($\mathbf{u}_l$) is the mean of the colors within kth (lth) superpixel, $s(\cdot)$ is the similarity of a pair of colors and λ is a parameter to control the weight of the two terms corresponding to the two objectives presented above. In Eq. (2), the more similar $\mathbf{u}_k$ and $\mathbf{d}_S(\tilde{y})$ are, the closer $\mathbf{g}'_k$ is to $\hat{\mathbf{g}}_{\tilde{y}}$. If the similarity of $\mathbf{u}_k$ and $\mathbf{d}_S(\tilde{y})$ is small, the second term plays a major role and $\mathbf{g}'_k$ will be determined by similar superpixels. Solving Eq. (2) is not difficult, which has a global minimum since we have $N << M$ and the function is quadratic.

After obtaining the optimal offset color vector $\mathbf{g}'_k$ for a superpixel $U(k)$, the mapped color of each pixel p within $U(k)$ in $\mathbf{I}_S$ is computed by $\mathbf{c}'_p = \mathbf{c}_p + \mathbf{g}'_k$, where $\mathbf{c}_p$ is the original color of pixel p. The soft mapping strategy preserves well the color similarity. As optimized mapping results are propagated directly from each superpixel to the corresponding pixels, block cases may still be generated. A solution is presented in the next section. The region highlighted by a yellow-dotted rectangle in Fig. 3(d) is an example.

6. $\mathscr{L}0$ Gradient Preservation

The $\mathscr{L}0$ gradient-preserving model is purposed to achieve image detail preservation by source image gradients. In this model, most pixel gradients remain unchanged but gradient changes of pixels along color region boundaries are allowed. Given the intermediate image, $\mathbf{I}_M$, and the source image gradients, $\nabla\mathbf{I}_S$, the model is expected to restore $\mathbf{I}_S$ details for the resulting image $\mathbf{I}_R$, while maximally keep color mapping procedure results. This goal can be translated into an optimization problem which minimizes the following energy function:

$$\|\mathbf{I}_R - \mathbf{I}_M\|_F^2 + \mu \|J(\nabla\mathbf{I}_R - \nabla\mathbf{I}_S)\|_0, \tag{3}$$

where $\mathbf{I}_M$, $\mathbf{I}_S$, and $\mathbf{I}_R$ denote the intermediate, source, and transferred images; ∇ is the gradient operator; $\|\cdot\|_0$ and $\|\cdot\|_F$ denote the $\mathscr{L}0$ and Frobenius norm, respectively; μ denotes $\mathscr{L}0$ norm weight; $J(\mathbf{A})$ is the operator denoting the L_2 norm square for matrix entry $\mathbf{A}$, i.e., $J(\mathbf{A})(i) = \|\mathbf{A}(i)\|_2^2$. The first term of Equation (3) keeps the mapped colors in $\mathbf{I}_M$. The second term enforces the pixels in $\mathbf{I}_R$ whose gradients equal to those in $\mathbf{I}_S$ to be as many as possible.

Equation (3) involves a $\mathscr{L}0$-norm regularized term known to be computationally intractable. Similar to [XLXJ11], an auxiliary variable $\mathbf{t}$ is introduced to rewrite the energy function as:

$$\|\mathbf{I}_R - \mathbf{I}_M\|_F^2 + \mu \|J(\mathbf{t})\|_0 + \nu \|\nabla\mathbf{I}_R - \nabla\mathbf{I}_S - \mathbf{t}\|_F^2, \tag{4}$$

where ν is a trade-off parameter. Equation (4) can be optimized using a block coordinate descent method [Tse01]. In each iteration, $\mathbf{t}$ and $\mathbf{I}_R$ are alternatively calculated. In the experiments, μ was set to 0.2 empirically. ν was initialized as 10μ and was doubled in each iteration until $\nu = 10^5$.

We fix $\mathbf{I}_R$ when computes $\mathbf{t}$. In initial case, $\mathbf{I}_R = \mathbf{I}_M$. Searching for an optimal solution for Equation (4) is equivalent to minimizing the following equation:

$$\frac{\mu}{\nu} \|J(\mathbf{t})\|_0 + \|\nabla\mathbf{I}_R - \nabla\mathbf{I}_S - \mathbf{t}\|_F^2, \tag{5}$$

which achieves its minimum when

$$\mathbf{t}(i) = \begin{cases} 0, & \|\nabla\mathbf{I}_R(i) - \nabla\mathbf{I}_S(i)\|_F^2 \le \frac{\mu}{\nu}; \\ \nabla\mathbf{I}_R(i) - \nabla\mathbf{I}_S(i), & otherwise. \end{cases} \tag{6}$$

Similarly, we fix $\mathbf{t}$ when computs $\mathbf{I}_R$. Searching for an optimal solution for Equation (4) is equivalent to minimizing the following equation:

$$\|\mathbf{I}_R - \mathbf{I}_M\|_F^2 + \nu \|\nabla\mathbf{I}_R - \nabla\mathbf{I}_S - \mathbf{t}\|_F^2. \tag{7}$$

The function in Equation (7) is quadratic and has a closed-form solution.

The resulting images from the $\mathscr{L}0$ gradient-preserving model and previous gradient-preserving model for a common input data

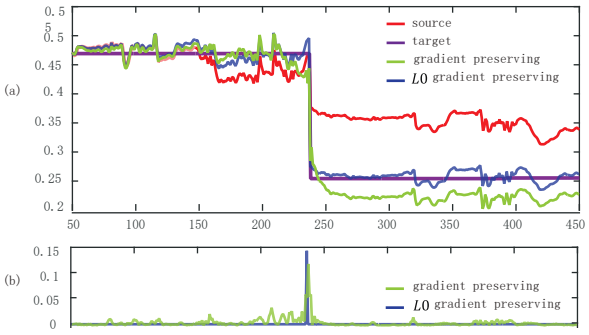

Figure 5: *Model analysis by an 1D signal from an image scanline. (a) Source signal (red), target signal (purple), resulting signals by gradient-preserving model(green) and $\mathscr{L}0$ gradient-preserving model (blue). (b) Green curve: gradient difference between red and green curve in (a); Blue curve: gradient difference between red and blue curve in (a).*

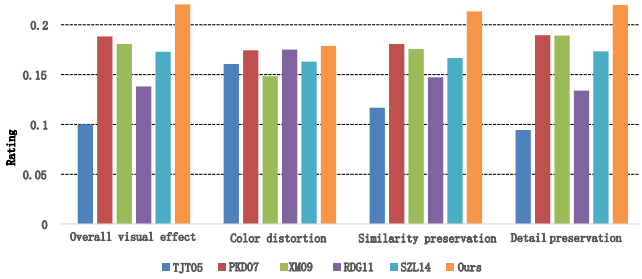

Figure 6: *Statistical analysis of overall performance. Five representative automatic approaches were compared to the proposed method for 84 source-target image pairs. We assessed the performance from following four aspects, overall visual effects, color distortion, detail preservation, and color similarity preservation. Each bar indicates a normalized rating of an performance aspect for an approach. A higher bar corresponds to more satisfactory visual performance.*

appear in Fig. 4. Image in Fig. 4(c) is visually superior to Fig. 4(e) especially at the color region boundaries. The pixel gradients at the boundaries change after color mapping, as the gradient analysis in Fig. 4(d). The gradient-preserving model tries to preserve the original gradients in Fig. 4(f). The advantage of the proposed $\mathscr{L}0$ gradient-preserving model is further analyzed using an 1D signal example which is a scanline from the source image in Fig. 4 shown in Fig. 5. The resulting signal produced by the $\mathscr{L}0$ gradient-preserving model is closer to the target signal than gradient-preserving model. In Fig. 5(b), the changed gradients occur throughout the resulting signals for gradient-preserving model. They sparsely exist at the edges of the resulting signal for the $\mathscr{L}0$ gradient-preserving model. It indicates that the resulting signals generated by the $\mathscr{L}0$ gradient-preserving model preserve the source signal gradients better than by gradient-preserving model.

7. Experimental Analysis

The section describes four sets of experiments to evaluate the effectiveness of the proposed method. The first experiment evaluated the performance of the proposed method and state-of-the-art automatic color transfer approaches. In the second experiment, the proposed method was compared to a state-of-the-art interactive method in [CFL*15]. It is classified as an interactive method as its system requires users to manually set dominant colors with target color palette. The last two sets of experiments were conducted to evaluate the proposed color mapping procedure and detail restoration procedure.

The proposed method was implemented with MATLAB. Each comparison method except for the one in [CFL*15] was evaluated using the MATLAB source code provided by the authors. These methods were run on a PC equipped with an Intel(R) Dual Core(TM) i7-6700HQ CPU @2.60GHz. The results by Chang et al. [CFL*15] were collected from the interactive system webpage. For the proposed method, the superpixel number N was empirically set to 1000 to obtain a trade-off between efficiency and performance. The parameters in the baseline methods were either interactively tuned to achieve the best results or set following the authors' suggestion.

7.1. Overall Performance

Automatic color transfer approaches In the first set of experiments for overall performance evaluation, 84 source-target image pairs were collected (each pair includes a source image and a target image) as the test examples. Some of these examples were from the experimental data of the comparison methods. The proposed method and five baseline methods, Tai et al. [TJT05], Pitie et al. [PKD07], Xiao et al. [XM09], Rabin et al. [RDG11], and Su et al. [SZL*14] were compared.

Forty participants, undergraduate or graduate students, majoring in computer science participated in the user study and collected a total of 32 valid user ratings for each input image pair. The results were evaluated for four aspects: a) overall visual effect; b) color distortion; c) color similarity preservation ; and d) detail preservation. For each aspect of a set of results, participants rated increasing satisfaction on a scale from 1 to 5. To avoid bias, the results of those methods were randomly arranged for each test example.

To compute the ratings of each aspect, we first sum up the scores of this aspect for each of the six methods, and then normalize the six sums by dividing with their total sum. In Fig. 6, the results of the statistical analysis of the collected user investigation data are given. The four histograms suggest the proposed method has achieved significantly better results in the overall visual effects, color similarity preservation, and detail preservation than the other methods. Fig. 7 shows some of the results produced by the comparison methods. Although the source and target images in the illustrated examples have very different color distributions, the proposed method produced good results, especially in color similarity preservation and detail preservation evaluation criteria.

Interactive color transfer approaches The second experiment compared the proposed method to the approach in [CFL*15]

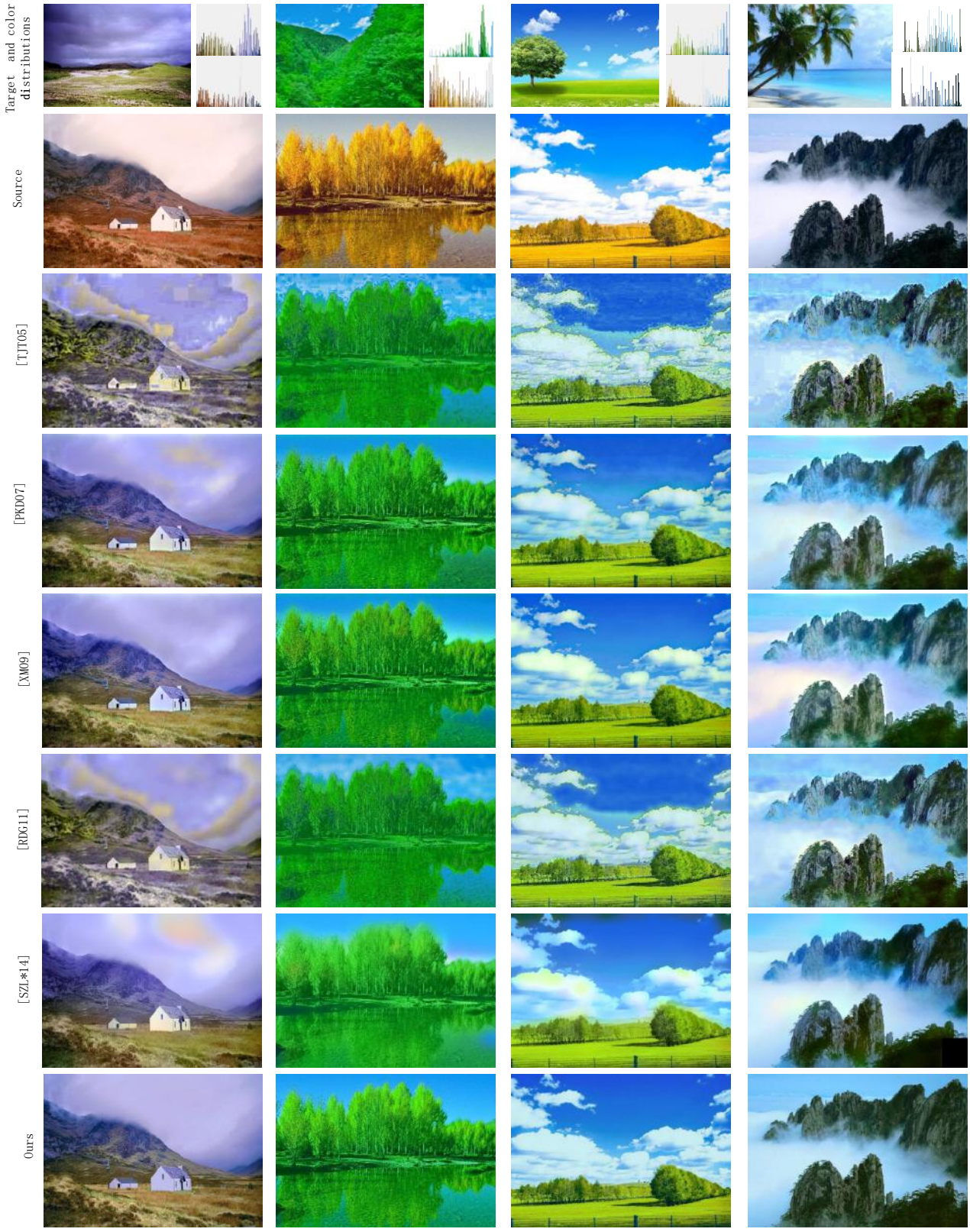

Figure 7: *Comparisons of the proposed method with Tai et al. [TJT05], Pitie et al. [PKD07] ($n = [10,10,3,3,10], \psi = 1$), Xiao et al. [XM09]($\lambda = 1$), Rabin et al. [RDG11], and Su et al. [SZL*14]. In the first row, the color distribution histograms of the target and source images are shown respectively at the top and bottom for each example.*

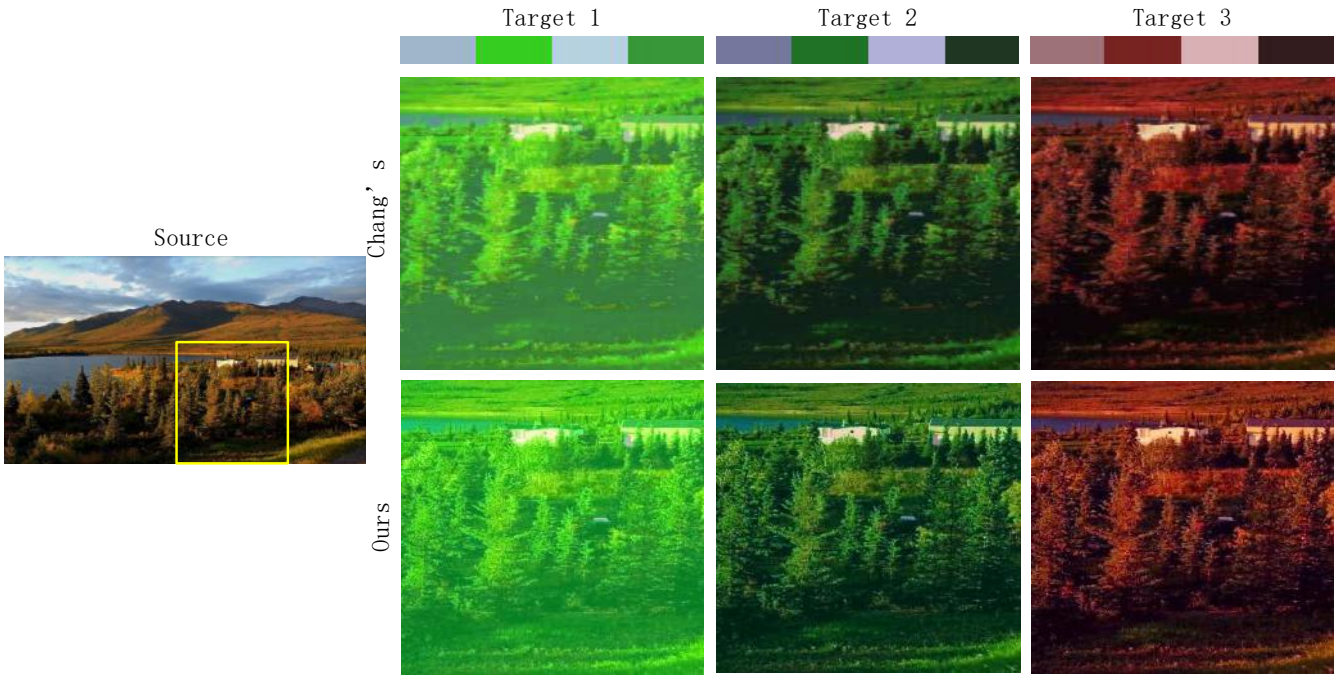

Figure 8: *Comparisons of the proposed method with the interactive approach in [CFL*15]. Given source image with a local region marked by yellow rectangle in the first column, the zoom-in resulting images of the marked region produced by [CFL*15] and ours are shown in last three columns. Our results are better to preserve image details. The corresponding target color palettes are shown on the top.*

Figure 9: *Influence of color mappings with different CC values on the resulting images produced by Chang et al. [CFL*15] and the proposed method. The provided several target color palettes generate different color consistencies. Smaller consistency CC corresponds to more satisfying resulting images for Chang's method. Our results have little effect on color consistency.*

which is a state-of-the-art interactive approach. The color transfer system allows the user to manually specify the input data (i.e., target dominant colors) via a color palette which differs from the automatic approaches.

In this experiment, 15 representative images were selected as source images. For each source image, a user was allowed to specify 3 sets of target dominant colors with the color palette. A representive example is shown in Fig. 8. A total of 15×3 comparison results were collected. After that, a user study similar to the first experiment was conducted on the results. Ninety-two participants made a quality judgement on assessment criteria of the overall visual effects for each of the 45 pairs of results. For each pair of results, a participant was asked to choose the one of higher quality they judged. Of the $15 \times 3 \times 92$ responses, 58.2% favored the proposed method. 41.8% preferred the approach in [CFL*15].

We also investigate how color consistency of mappings between source dominant colors and target dominant colors impacts the quality of results. In Fig. 9 five target color palettes were provided which generated different color consistencies. The color consistencies were given in Fig. 9. The experiment found that the results by the approach in [CFL*15] are with qualities close to ours when the color consistency is small. Otherwise their visual effects were more deteriorated than ours.

7.2. Color Mapping Evaluation

The similarity-preserving color mapping model was compared with three existing representative schemes to measure performance. They are GMM blending model [TJT05], color histograms matching [XM09] and probabilistic color mapping [SZL*14] separately. All four schemes were tested on 50 examples. In each

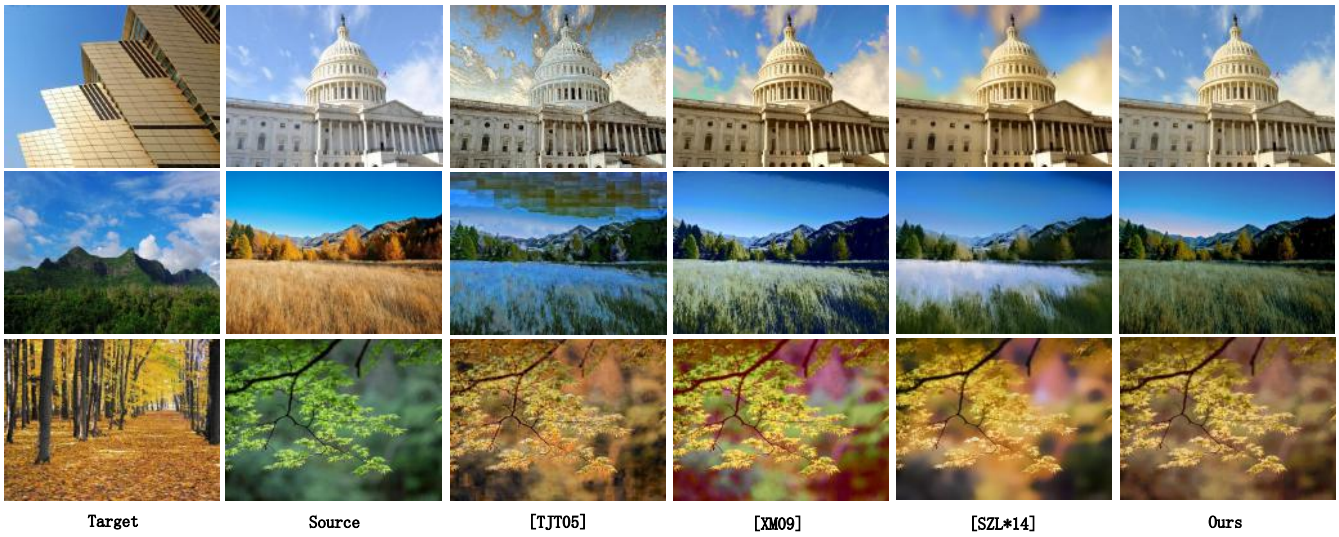

Figure 10: *Color mapping comparisons. The proposed color mapping scheme is compared with those using GMM blending model [TJT05], color histogram matching [XM09], and probabilistic color mapping [SZL*14].*

scheme, an intermediate image was generated by conducting only the color mapping step on an input image pair.

Fig. 10 shows three representative examples. The balance of the results are in the supplemental material. The results generated by the proposed scheme appear to have superior visual effects compared to those of the other schemes on these examples. The visual effect of the results produced by the GMM blending based scheme is relatively inferior compared to the other schemes. e.g. the top row sky, the grass and sky in the middle row, and the bottom row maple leaves. The regions with inferior visual effects mainly suffer from color inconsistencies. In their color mapping step, color similarities between pixels are not preserved, so their results have the problem of color inconsistency.

7.3. Detail Preservation Evaluation

In this set of experiments, the advantages of the proposed $\mathscr{L}0$ gradient-preserving model in detail preservation was studied. Two representative existing models, gradient-preserving [XM09] and Yaroslavsky filter [RDG11], were used as the baseline. Twenty sets of intermediate images produced by the color mapping procedure and the corresponding source images were used as the input for each comparison model. In the three models, pixel reference color is from the intermediate image and its reference detail information is from the source image.

The results generated by the three models were compared for all the test examples. The proposed $\mathscr{L}0$ gradient-preserving model and gradient-preserving model had better visual performance than the Yaroslavsky filter in detail restoration. The Yaroslavsky filter model results are relatively more blurry than those of the $\mathscr{L}0$ gradient-preserving model. See the resulting trees in the fist row and the grass in the second row in Fig 11. In addition, $\mathscr{L}0$ gradient-preserving model produced more natural results around color region boundaries compared to gradient-preserving model, e.g. the boundary of mountain and sky in the fist row and the boundary of grass and sky in the second row in Fig 11.

7.4. Timing

The primary computational cost of the proposed approach is the iterative optimization of $\mathscr{L}0$ gradient-preserving model and the segmentation process for superpixels. In the current MATLAB-based implementation, a Fast Fourier Transform (FFT) was used to accelerate solving Equation (7). The iterative optimization takes about 3 seconds for 800×600 input images. The segmentation process takes 3 seconds. The entire color transfer method takes about 9 seconds to produce the final result for an 800×600 input image.

7.5. Limitations

The overall visual quality of the generated results is effected by dominant color extraction. As all dominant color based methods, their success depends on obtaining ideal dominant colors. They are robust within a large range of dominant color number selection. However, in the interactive color editing mode, the minimum number of dominant colors is preferred to reduce the interaction for appropriate target colors via color palette. It is not easy to determine the best dominant color number. For example, there are three visually primary colors containing green in images in Fig. 12. However, when the dominant color number is set to 3, green fails to serve as a dominant color during the clustering procedure. When the dominant color number is changed to 5, all primary colors are obtained and an ideal image is produced.

Semantic analysis may be added to improve the proposed method in some limited cases. For example, for a source image containing a scene with few and similar colors, our method may

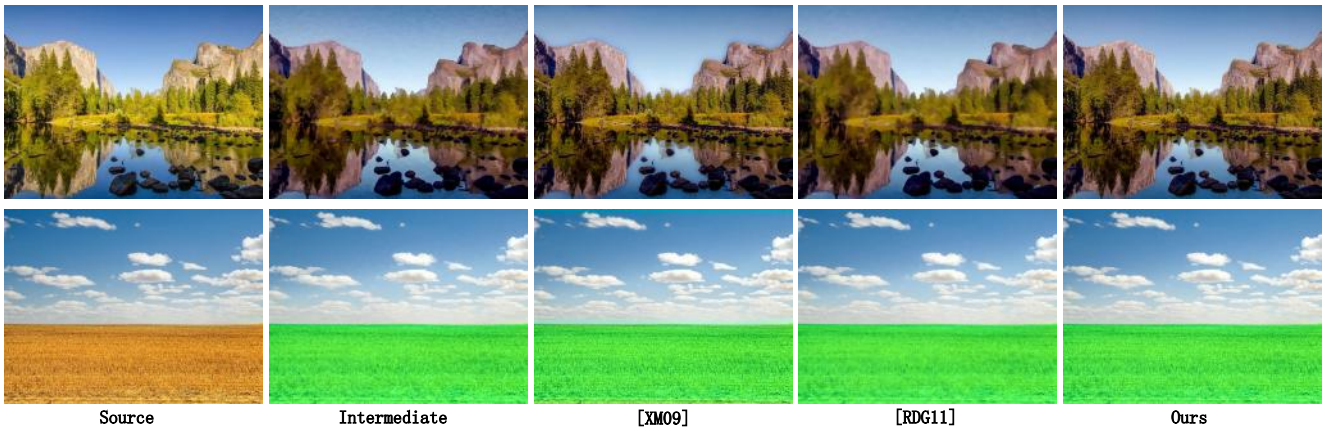

Figure 11: *Detail preservation comparisons. From the left the first two columns show the source and intermediate images (i.e., the color mapping procedure output); the next three columns show the results produced by three models: gradient-preserving [XM09], Yaroslavsky filter [RDG11] and the proposed $\mathscr{L}0$ gradient-preserving. The intermediate image provides pixel reference colors for the three models.*

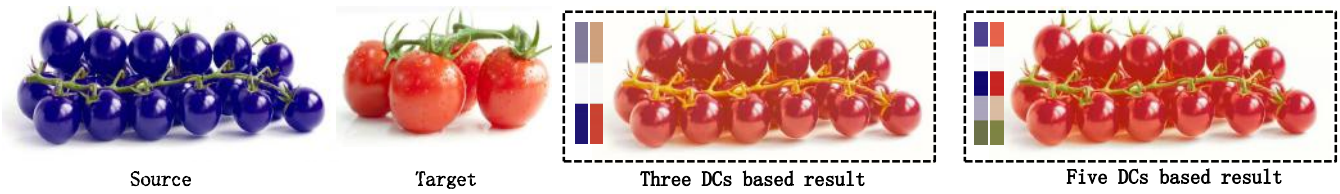

Figure 12: *The effect of dominant color clustering on the results. If the clustering number is set too small, such as three rather than five, the method may produce inferior visual effects because green is not a dominant color at a setting of three.*

generate undesirable results due to the noise generated when segmenting a source image into super-pixels. A more powerful segmentation algorithm which uses semantic information might improve the proposed method in these cases. It is possible in some cases that the scenes of a source image could only be mapped to some special target colors, such as a shadow in the source image. The proposed method cannot achieve this function automatically.

8. Conclusions

Color transfer is an important and challenging research problem. Successful color transfers should meet several basic criteria: accurately conveying the colors in the target image to the source images while maintaining source color similarity, and preserving source image details. The proposed method addresses these problems well, even if source and target image colors are not well matched.

The proposed similarity-preserving color mapping model emphasizes retaining source image pixel color similarity while matching target dominant colors. Pixel color similarity is achieved by combining local with global pixel color similarity to simplify the model solver. Each superpixel is as a sample because the local pixels in a superpixel with similar colors follow the same color mapping mode. Based on superpixels, the similarity-preserving color mapping model is established to achieve global color similarity. The proposed scheme produces better results over a large number of test examples than those used by previous methods.

In most cases it is impossble to preserve all image gradients during color transfer due to different color mapping modes for different dominant colors. The proposed $\mathscr{L}0$ gradient-preserving method enforces pixels within color regions in the resulting image to have the same gradients as the corresponding pixels in the source image. It allows sparse pixel gradients to change along color region boundaries. The proposed $\mathscr{L}0$ gradient-preserving method does not have the edge blur or color blending appearance caused by globally gradient-preserving schemes.

We expect the proposed method can accurately obtain dominant colors consistent with human visual perception. It should greatly simplify the interactive editing process. The best case scenario would be a one-to-one correspondence between the visually primary colors in the source image and the dominant colors provided either automatically or via user interaction. A semantic analysis of image details is worth considering which may extend the application scope of this method.

Acknowledgements

We thank all the reviewers for their valuable comments and feedback. This work was supported in part by grants from the National Natural Science Foundation of China (Grant No. U1301253, 61572202, 61602183, 61472455), the Science and

Technology Plan Project of Hunan Province (2016TP1020), the Program of Key Disciplines in Hunan Province and Fundamental Research Funds for the Central Universities ("Research on Fundamental Problems of Dynamic Geometries").

References

[BSPP13] BONNEEL N., SUNKAVALLI K., PARIS S., PFISTER H.: Example-based video color grading. *ACM Transactions on Graphics (TOG) 32*, 4 (2013), 39. 3

[CFL*15] CHANG H., FRIED O., LIU Y., DIVERDI S., FINKELSTEIN A.: Palette-based photo recoloring. *ACM Transactions on Graphics (Proc. SIGGRAPH)* (2015). 1, 2, 6, 8

[CZL14] CHENG X., ZENG M., LIU X.: Feature-preserving filtering with l_0 gradient minimization. *Computer & Graphics 38*, 2 (2014), 150–157. 3

[DZ13] DONG B., ZHANG Y.: An efficient algorithm for l_0 minimization in wavelet frame based image restoration. *Journal of Scientific Computing 54*, 2-3 (2013), 350–368. 3

[HLKK14] HWANG Y., LEE J.-Y., KWEON I. S., KIM S. J.: Color transfer using probabilistic moving least squares. In *CVPR* (2014), pp. 3342–3349. 2

[HS13] HE L., SCHAEFER S.: Mesh denoising via l_0 minimization. *ACM Transactions on Graphics (TOG) 32*, 4 (2013), 64. 3

[HSGL11] HACOHEN Y., SHECHTMAN E., GOLDMAN D. B., LISCHINSKI D.: Non-rigid dense correspondence with applications for image enhancement. *ACM Transactions on Graphics (TOG) 30*, 4 (2011), 70:1–70:9. 2

[LPSB17] LUAN F., PARIS S., SHECHTMAN E., BALA K.: Deep photo style transfer. *arXiv preprint arXiv:1703.07511* (2017). 2

[LTRC11] LIU M., TUZEL O., RAMALINGAM S., CHELLAPPA R.: Entropy rate superpixel segmentation. In *The 24th IEEE Conference on Computer Vision and Pattern Recognition, CVPR 2011, Colorado Springs, CO, USA, 20-25 June 2011* (2011), pp. 2097–2104. 5

[Mac67] MACQUEEN J.: Some methods for classification and analysis of multivariate observations. In *In 5-th Berkeley Symposium on Mathematical Statistics and Probability* (1967), pp. 281–297. 4

[NKB14] NGUYEN R., KIM S., BROWN M.: Illuminant aware gamut-based color transfer. *Computer Graphics Forum 33*, 7 (2014), 319–328. 2

[NRS15] NGUYEN C. H., RITSCHEL T., SEIDEL H.-P.: Data-driven color manifolds. *ACM Transactions On Graphics 34*, 2 (2015). 2

[PKD05] PITIE F., KOKARAM A. C., DAHYOT R.: N-dimensional probability density function transfer and its application to color transfer. In *ICCV* (2005), pp. 1434–1439. 2

[PKD07] PITIÉ F., KOKARAM A. C., DAHYOT R.: Automated colour grading using colour distribution transfer. *Computer Vision and Image Understanding 107*, 1 (2007), 123–137. 1, 2, 6, 7

[PR11] POULI T., REINHARD E.: Progressive color transfer for images of arbitrary dynamic range. *Computers & Graphics 35*, 1 (2011), 67–80. 2

[QL15] QIAN LIU CAIMING ZHANG Q. G. A. Y. Z.: A nonlocal gradient concentration method for image smoothing. *Computational Visual Media 1*, 3 (2015), 197–209. 3

[RAGS01] REINHARD E., ADHIKHMIN M., GOOCH B., SHIRLEY P.: Color transfer between images. *IEEE Computer Graphics and Applications 21*, 5 (2001), 34–41. 2

[RDG11] RABIN J., DELON J., GOUSSEAU Y.: Removing artefacts from color and contrast modifications. *IEEE Transactions on Image Processing 20*, 11 (2011), 3073–3085. 2, 3, 6, 7, 9, 10

[RG00] RUBNER Y. T. C., GUIBAS L. J.: The earth mover's distance as a metric for image retrieval. *Int. J. Comput. Vision 40*, 2 (2000), 99–121. 4

[SCHP12] SHEN C.-T., CHANG F.-J., HUNG Y.-P., PEI S.-C.: Edge-preserving image decomposition using l_1 fidelity with l_0 gradient. In *SIGGRAPH Asia 2012 Technical Briefs* (2012), p. 6. 3

[SPLM15] SHAO-PING LU GUILLAUME DAUPHIN G. L., MUNTEANU A.: Color retargeting: Interactive time-varying color image composition from time-lapse sequences. *Computational Visual Media 1*, 4 (2015), 321–330. 1

[SZL*14] SU Z., ZENG K., LIU L., LI B., LUO X.: Corruptive artifacts suppression for example-based color transfer. *IEEE Transactions on Multimedia 16*, 4 (2014), 988–999. 1, 2, 3, 6, 7, 8, 9

[TJT05] TAI Y.-W., JIA J., TANG C.-K.: Local color transfer via probabilistic segmentation by expectation-maximization. In *CVPR* (2005), pp. 747–754. 1, 2, 6, 7, 8, 9

[TJT07] TAI Y.-W., JIA J., TANG C.-K.: Soft color segmentation and its applications. *IEEE Transactions on Pattern Analysis and Machine Intelligence 29*, 9 (2007), 1520–1537. 2

[TM98] TOMASI C., MANDUCHI R.: Bilateral filtering for gray and color images. In *ICCV* (1998), pp. 839–846.

[Tse01] TSENG P.: Convergence of a block coordinate descent method for nondifferentiable minimization. *Journal of Optimization Theory and Applications 109*, 3 (2001), 475–494. 5

[WDK*13] WU F., DONG W., KONG Y., MEI X., PAUL J., ZHANG X.: Content-based colour transfer. *Computer Graphics Forum 32*, 1 (2013), 190–203. 2

[WYW*10] WANG B., YU Y., WONG T.-T., CHEN C., XU Y.-Q.: Data-driven image color theme enhancement. *ACM Transactions on Graphics (TOG) 29*, 6 (2010), 146:1–10. 2

[WYX11] WANG B., YU Y., XU Y.-Q.: Example-based image color and tone style enhancement. *ACM Transactions on Graphics (TOG) 30*, 4 (2011), 64:1–12. 2

[XLH15] XUJIE LI HANLI ZHAO G. N., HUANG H.: Image recoloring using geodesic distance based color harmonization. *Computational Visual Media 1*, 2 (2015), 143–155. 2

[XLXJ11] XU L., LU C., XU Y., JIA J.: Image smoothing via l_0 gradient minimization. *ACM Transactions on Graphics (TOG) 30*, 6 (2011), 174. 3, 5

[XM09] XIAO X., MA L.: Gradient-preserving color transfer. *Computer Graphics Forum 28*, 7 (2009), 1879–1886. 1, 2, 6, 7, 8, 9, 10

[YPCL13] YOO J.-D., PARK M.-K., CHO J.-H., LEE K. H.: Local color transfer between images using dominant colors. *Journal of Electronic Imaging 22*, 3 (2013), 033003. 1, 2

[ZDL13] ZHANG Y., DONG B., LU Z.: l_0 minimization for wavelet frame based image restoration. *Mathematics of Computation 82*, 282 (2013), 995–1015. 3

[ZZZG14] ZHANG J., ZHAO C., ZHAO D., GAO W.: Image compressive sensing recovery using adaptively learned sparsifying basis via l_0 minimization. *Signal Processing 103* (2014), 114–126. 3